PROCEEDINGS OF SPIE

Growth and spectroscopy of Er3+-doped Na5Y9F32 (5NaF·9YF3) crystal

Basyrova, Liza, Loiko, Pavel, Doualan, Jean-Louis, Benayad, Abdelmjid, Zin Elabedine, Ghassen, et al.

SPIE.

Event: SPIE Photonics Europe, 2022, Strasbourg, France

Growth and spectroscopy of Er³⁺-doped Na₅Y₉F₃₂ (5NaF·9YF₃) crystal

Liza Basyrova[a,*], Pavel Loiko[a], Jean-Louis Doualan[a], Abdelmjid Benayad[a], Ghassen Zin Elabedine[b], Rosa Maria Solé[b], Magdalena Aguiló[b], Francesc Díaz[b], Xavier Mateos[b,#], Elena Dunina[c], Alexey Kornienko[c], Alain Braud[a], Christophe Labbé[a], and Patrice Camy[a]

[a]Centre de recherche sur les Ions, les Matériaux et la Photonique (CIMAP), UMR 6252 CEA-CNRS-ENSICAEN, Université de Caen Normandie, 6 Boulevard Maréchal Juin, 14050 Caen Cedex 4, France
[b]Universitat Rovira i Virgili, Physics and Cristallography of Materials (FiCMA), Marcel·li Domingo, 1, 43007 Tarragona, Spain. [#]Serra Húnter Fellow
[c]Vitebsk State Technological University, 72 Moskovskaya Ave., 210035 Vitebsk, Belarus

ABSTRACT

We report on the growth, structure and spectroscopy of an Er³⁺-doped Na₅Y₉F₃₂ (5NaF·9YF₃) crystal featuring significant inhomogeneous spectral broadening. Single-crystals of Na₅Y₉F₃₂ doped with 0.22 – 9.63 at.% Er³⁺ were grown by the Czochralski method. Er:Na₅Y₉F₃₂ exhibits a cubic fluorite-type structure (a = 5.4881(2) Å for 5.59 at.% Er³⁺ doping). The most intense Raman band of this material is found at ~404 cm⁻¹. Er³⁺ ions in Na₅Y₉F₃₂ exhibit a broad and smooth emission band owing to the $^4I_{11/2} \rightarrow {}^4I_{13/2}$ transition with a maximum stimulated-emission cross-section of 0.42×10^{-20} cm² at 2708 nm. According to the Judd-Ofelt analysis, the radiative lifetime of the $^4I_{11/2}$ multiplet is 10.0 ms and the luminescence branching ratio $\beta(^4I_{11/2} \rightarrow {}^4I_{13/2})$ is 17.6%. The luminescence lifetimes of the $^4I_{11/2}$ and $^4I_{13/2}$ Er³⁺ states were studied as a function of the doping concentration. For 5.59 at.% Er doping, they are 7.72 ms and 6.69 ms, respectively, representing a favorable ratio for mid-infrared laser operation.

Keywords: fluoride crystals, sodium-yttrium fluoride, Czochralski method, erbium ions, optical spectroscopy.

1. INTRODUCTION

Crystalline materials formed in binary systems of alkali metal fluorides – rare-earth trifluorides have a good potential as laser host matrices. One example is the NaF – YF₃ binary system. Thoma *et al.* first studied this system and determined the existence of a cubic solid-solution with composition 5NaF·9YF₃ (Na₅Y₉F₃₂) and relatively low melting point at 975 °C [1,2]. Generally, Na₅Y₉F₃₂ is a member of a family of double sodium-yttrium fluoride solid-solution crystals with a general chemical formula of Na₀.₅₋ₓY₀.₅₊ₓF₂₊₂ₓ [3]. Na₅Y₉F₃₂ crystallizes in the cubic class exhibiting a fluorite-type structure (fluorite is the mineral form of CaF₂), even though both components of the binary system (NaF, YF₃) do not exhibit such a structure. The dopant rare-earth ions (RE³⁺) replace for the Y³⁺ ones in the Na₅Y₉F₃₂ lattice. The local symmetry of the surrounding of the Y³⁺ ions (and thus also RE³⁺ ones) is C₄ᵥ [4]. There are three non-equivalent positions for fluorine anions (F⁻) in Na₅Y₉F₃₂. Previous studies indicate that in Na₀.₅₋ₓY₀.₅₊ₓF₂₊₂ₓ solid-solutions with $x = 0$ - 0.14, cuboctahedral clusters Y₆F₃₆₋₃₈ are formed [5,6]. This induces a significant inhomogeneous spectral broadening for the dopant RE³⁺ ions leading to smooth and broad absorption and emission spectra (a "glassy-like" spectral behavior) [7]. It is of great interest for broadly tunable and mode-locked lasers.

Erbium ions (Er³⁺) are attractive for laser emission in the mid-infrared, at 2.8 μm, according to the $^4I_{11/2} \rightarrow {}^4I_{13/2}$ electronic transition. ~2.8 μm lasers are of practical importance for laser surgery. Fluoride crystals are attractive for heavy doping with Er³⁺ ions for mid-infrared laser applications [8-11]. Among them, Er:CaF₂ is of particular interest because of the profound rare-earth ion clustering leading to both i) efficient energy-transfer upconversion between the Er³⁺ ions within clusters even at moderate doping levels and ii) broadband emission properties [11,12]. It would be interesting to explore the potential of Er³⁺-doped fluorite-type Na₅Y₉F₃₂ crystals as laser gain media.

*e-mail: liza.basyrova@ensicaen.fr

So far, only a few studies were dedicated to rare-earth doped $Na_{0.5-x}Y_{0.5+x}F_{2+2x}$ crystals as laser gain media. Tkachuk *et al.* reported on the mid-infrared laser operation of an Er^{3+}-doped $Na_{0.4}Y_{0.6}F_{2.2}$ ($2NaF\cdot3YF_3$) crystal [13]. Under pumping by an InGaAs laser diode, an output power of 72 mW at 2.8 µm was achieved with a slope efficiency of only 4%. Excited-state absorption of Er^{3+} ions in $Na_5Y_9F_{32}$ crystals was studied in [14].

In the present work, we report on the growth, structural and spectroscopic study of a disordered Er^{3+}-doped $Na_5Y_9F_{32}$ crystal promising for the development of ~2.8 µm lasers.

2. EXPERIMENTAL

2.1 Crystal growth

Single-crystals of $Na_5Y_9F_{32}$ ($5NaF\cdot9YF_3$) doped with 0.2 – 10 at.% Er^{3+} (with respect to Y^{3+}, initial composition) were grown by the Czochralski (Cz) method. The growth charge was prepared from a stoichiometric mixture of NaF (purity: 2N), YF_3 and ErF_3 reagents. The rare-earth fluorides (REF_3) were obtained via fluorination of the corresponding oxides (RE_2O_3, 4N) using an excess of NH_4HF_2 solution under heating at 180 °C and the dry cakes were annealed at 650 °C for 4 h under Ar atmosphere to remove the residual NH_4F and moisture. The growth charge was well degassed in a vacuum furnace (10^{-5} mbar) by gradual heating up to 300 °C. The crucible was then heated to the temperature slightly higher than the melting point of $Na_5Y_9F_{32}$ (975 °C) under an Ar + CF_4 atmosphere to ensure that the raw materials are completely molten. For the crystal growth, an oriented seed from undoped $Na_5Y_9F_{32}$ was used. The pulling rate was 3 mm/h.

The as-grown crystals had a cylindrical shape with uniform cross-section (Φ12- 15 mm, length: 20 - 25 mm). All the crystals, except the one with the highest doping (10 at.% Er^{3+}), were transparent and free of cracks and inclusions. The crystals had a rose coloration due to the Er^{3+} dopant. The actual Er^{3+} doping level was determined by atomic emission spectroscopy (AES): five crystals doped with 0.22, 1.16, 2.0, 5.59 and 9.63 at.% Er^{3+} were studied. E.g., for the 5.59 at.% Er^{3+}-doped crystal, the corresponding ion density N_{Er} was 8.23×10^{20} at/cm^3.
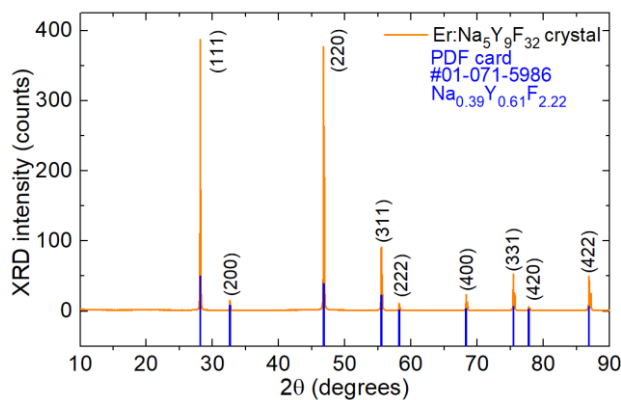

Figure 1. A photograph of a polished 2.0 at.% $Er:Na_5Y_9F_{32}$ crystal.

Figure 2. X-ray powder diffraction (XRD) pattern of a 5.59 at.% $Er:Na_5Y_9F_{32}$ crystal, *blue peaks* – theoretical reflections for undoped $Na_{0.39}Y_{0.61}F_{2.22}$ (PDF card #01-071-5986), *numbers* – Miller's indices (*hkl*).

The phase purity and the crystal structure were confirmed by X-ray powder diffraction (XRD). The XRD pattern was measured with a D8-Advance diffractometer with a lynx-eye detector (opening 2.9463º) using Cu Kα1 (λ = 1.5418 Å) radiation in the 2θ range of 10 – 90° with a step size of 0.02° and a step time of 2 s. The measured XRD pattern for the

5.59 at.% $Er:Na_5Y_9F_{32}$ crystal is shown in Fig. 2. No other peaks except those belonging to the cubic phase ($Na_{0.39}Y_{0.61}F_{2.22}$, ICSD card #01-071-5986) were found. The crystal structure of $Er:Na_5Y_9F_{32}$ was refined by the Rietveld method using the Topas software. $Er:Na_5Y_9F_{32}$ belongs to the cubic class (sp. gr. O_h^5 - *Fm-3m*, No. 225) being isostructural to CaF_2. The calculated lattice constant $a = 5.4881(2)$ Å (the number of formula units in the unit-cell $Z = 4$), the volume of the unit-cell $V = 165.299(3)$ Å^3 and the calculated density $\rho_{calc} = 3.888$ g/cm^3.

3. RESULTS AND DISCUSSION

3.1 Raman spectra

The Raman spectra of an undoped and 0.22 at.% Er^{3+}-doped $Na_5Y_9F_{32}$ crystals were measured using a confocal microscope (inVia, Renishaw) equipped with a ×50 objective (Leica) and an Ar^+ ion laser (457, 488 nm), see Fig. 3. The Raman spectrum of the undoped $Na_5Y_9F_{32}$ crystal exhibits several broad poorly resolved bands with the maxima at 130, 229, 350, 404, 470 and 516 cm^{-1}. The most intense band is found at 404 cm^{-1}. For the 0.22 at.% Er^{3+}-doped crystal, the Raman bands overlap with the Er^{3+} luminescence. Despite this, a similar set of Raman-active modes is observed. The low phonon energy behavior of the $Na_5Y_9F_{32}$ host matrix is advantageous for Er^{3+} doping with the goal of observing mid-IR emission.
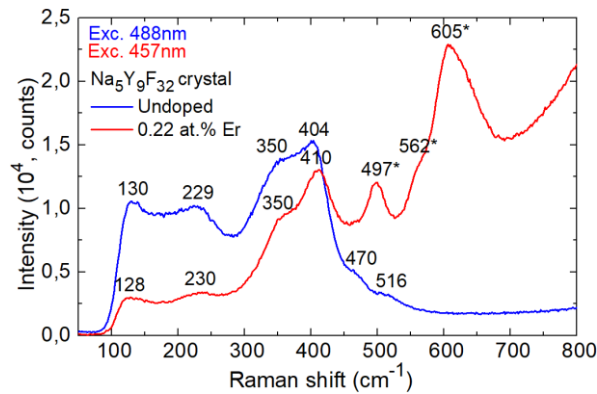

Figure 3. Unpolarized Raman spectra of undoped *(blue)* and 0.22 at.% Er doped *(red)* $Na_5Y_9F_{32}$ crystals, *numbers* denote the Raman frequencies in cm^{-1}.

3.2 Optical absorption

The absorption spectrum of the 5.59 at.% $Er:Na_5Y_9F_{32}$ crystal was measured using a spectrophotometer (Lambda 1050, Perkin Elmer), Fig. 4(a). The absorption bands are related to transitions of Er^{3+} ions from the ground-state, $^4I_{15/2}$, to excited-states ranging from $^4I_{13/2}$ up to $^2G_{7/2}$. Here, the assignment is after Carnall *et al.* [15].
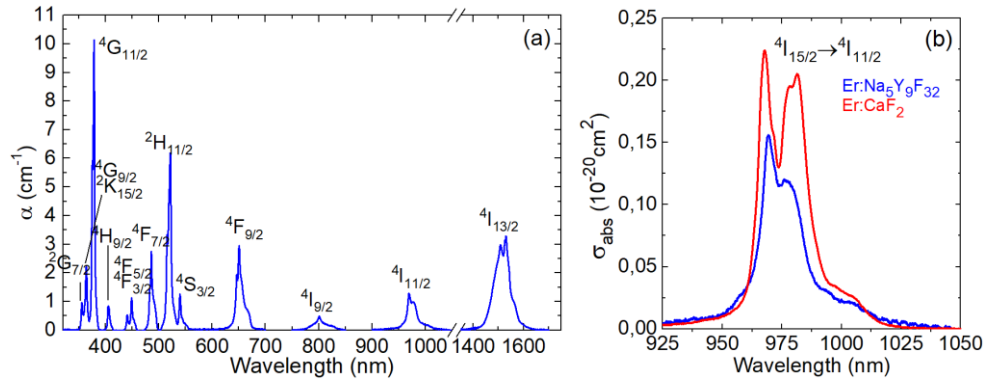

Figure 4. (a) An overview absorption spectrum of a 5.59 at.% $Er:Na_5Y_9F_{32}$ crystal; (b) absorption cross-section spectra for the $^4I_{15/2} \rightarrow {}^4I_{11/2}$ transition of Er^{3+} ions in the $Na_5Y_9F_{32}$ and CaF_2 cubic crystals.

For the $^4I_{15/2} \rightarrow {}^4I_{11/2}$ transition which is typically used for pumping of Er^{3+}-doped materials, e.g., by using commercial InGaAs laser diodes, the peak absorption cross-section ($\sigma_{abs} = \alpha_{abs}/N_{Er}$) is 0.16×10^{-20} cm^2 at 969.3 nm corresponding to a

large absorption bandwidth (full width at half maximum) of ~18 nm, see Fig. 4(b). As compared to another cubic crystal exhibiting a "glassy-like" spectroscopic behavior, Er:CaF$_2$, Fig. 4(b), Er:Na$_5$Y$_9$F$_{32}$ provides lower absorption cross-sections while less structured absorption band. The broadband absorption properties of Er:Na$_5$Y$_9$F$_{32}$ are of practical importance for diode-pumping.

The transition intensities of Er^{3+} ions in Na$_5$Y$_9$F$_{32}$ were determined based in the framework of the standard Judd-Ofelt (J-O) theory based on the measured absorption spectrum [16,17]. The obtained intensity parameters are $\Omega_2 = 2.314$, $\Omega_4 = 0.673$ and $\Omega_6 = 1.002$ [10^{-20} cm^2]. Using these parameters, the probabilities of spontaneous radiative transitions $A^{\Sigma}_{calc}(JJ')$, the luminescence branching ratios $\beta(JJ')$ and the radiative lifetimes of the excited-states τ_{rad} were then calculated, Table 1. For the upper laser manifold ($^4I_{11/2}$), the radiative lifetime is as long as 9.99 ms and the luminescence branching ratio corresponding to emission in the mid-IR, $\beta(^4I_{11/2} \rightarrow {}^4I_{13/2})$ is relatively high, 17.6%.

Table 1. Probabilities of spontaneous radiative transitions of Er^{3+} ions in Na$_5$Y$_9$F$_{32}$ calculated using the standard J-O theory ($<\lambda_{em}>$ - mean emission wavelength, $\beta(JJ')$ – luminescence branching ratios, $A^{\Sigma}_{calc}(JJ')$ –probabilities of radiative transitions, ED: electric dipole, MD: magnetic dipole, A_{tot} – total probabilities, τ_{rad} – radiative lifetimes).

Transition J → J'		$<\lambda_{em}>$, nm	$\beta(JJ')$	$A^{\Sigma}_{calc}(JJ')$, s^{-1}	A_{tot}, s^{-1}	τ_{rad}, ms
$^4I_{13/2} \rightarrow$	$^4I_{15/2}$	1532.3	1.000	63.22^{ED} +31.98^{MD}	95.20	10.50
$^4I_{11/2} \rightarrow$	$^4I_{13/2}$ $^4I_{15/2}$	2745.7 983.5	0.176 0.824	10.48^{ED} +7.12^{MD} 82.45^{ED}	100.05	9.99

3.3 Mid-infrared luminescence

The spectra of mid-IR luminescence were measured using an optical spectrum analyzer (Yokogawa AQ6376E) purged with N$_2$ gas to diminish the effect of the structured water vapor absorption in air and a zirconium fluoride (ZrF$_4$) fiber. As an excitation source, we used a Ti:Sapphire laser tuned to 970 nm. The stimulated-emission (SE) cross-sections, σ_{SE}, for the $^4I_{11/2} \rightarrow {}^4I_{13/2}$ transition of Er^{3+} ions in the Na$_5$Y$_9$F$_{32}$ crystal were calculated using the Füchtbauer–Ladenburg (F-L) formula [18]:

$$\sigma_{SE}(\lambda) = \frac{\lambda^5}{8\pi <n>^2 \tau_{rad}c} \frac{\beta(JJ')W'(\lambda)}{\int \lambda W'(\lambda)d\lambda},$$

where, λ is the light wavelength, $<n>$ is the refractive index at the mean emission wavelength $<\lambda_{em}>$, τ_{rad} is the radiative lifetime of the emitting state ($^4I_{11/2}$) and $\beta(JJ')$ is the branching ratio, c is the speed of light and $W'(\lambda)$ is the luminescence spectrum corrected for the spectral response of the set-up. For the Er:Na$_5$Y$_9$F$_{32}$ crystal, $<n> = 1.470$, $\tau_{rad} = 9.99$ ms and $\beta(JJ') = 17.6\%$, according to the Judd-Ofelt analysis, cf. Table 1.
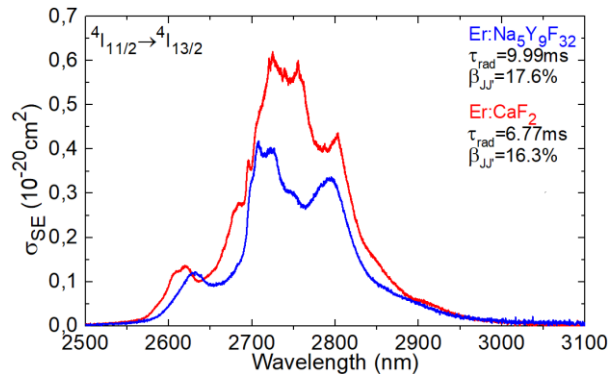

Figure 5. Stimulated-emission (SE) cross-sections, σ_{SE}, for the $^4I_{11/2} \rightarrow {}^4I_{13/2}$ transition of Er^{3+} ions in the Na$_5$Y$_9$F$_{32}$ and CaF$_2$ cubic crystals.

The calculated σ_{SE} spectrum for the Er:Na$_5$Y$_9$F$_{32}$ crystal is shown in Fig. 5. This material exhibits a broad and smooth emission band (a "glassy"-like behavior) spanning from 2.55 to 3.05 μm with a maximum $\sigma_{SE} = 0.42 \times 10^{-20}$ cm^2 at 2708

nm and another intense peak at a longer wavelength, 2795 nm (σ_{SE} = 0.33×10^{-20} cm^2). For comparison, in the same figure, we show the σ_{SE} spectrum for the Er:CaF$_2$ crystal. The spectra of both crystals are similar in shape. Due to the longer radiative lifetime of the $^4I_{11/2}$ Er^{3+} state in Na$_5$Y$_9$F$_{32}$, the absolute values of SE cross-sections for this material are lower than those for Er:CaF$_2$.

3.4 Luminescence dynamics

The luminescence dynamics was studied employing a ns optical parametric oscillator (Horizon, Continuum), a 1/4 m monochomator (Oriel 77200), a fast InGaAs detector and an 8 GHz digital oscilloscope (DSA70804B, Tektronix). The decay curves of luminescence from the $^4I_{11/2}$ and $^4I_{13/2}$ states of Er^{3+} ions in the 5.59 at.% Er:Na$_5$Y$_9$F$_{32}$ crystal measured under resonant excitation are shown in Fig. 6 plotted in a semi-log scale. The luminescence decay was studied using finely powdered crystal samples to reduce the effect of radiation trapping (reabsorption). The luminescence decay times τ_{lum} amount to 7.72 ms ($^4I_{11/2}$) and 6.69 ms ($^4I_{13/2}$), representing a favorable ratio for mid-IR laser operation.

Table 2 summarizes the τ_{lum} values as a function of the Er^{3+} doping concentration. At a very low doping level (0.22 at.% Er^{3+}), the lifetime of the lowest excited-state, $^4I_{13/2}$, is close to the radiative value determined using the J-O theory. For the next excited state, $^4I_{11/2}$, the τ_{lum} values is relatively close to the radiative lifetime indicating a weak non-radiative relaxation in agreement with the low phonon energy behavior of the host matrix. Upon Er^{3+} doping, the $^4I_{13/2}$ lifetime decreases fast while the $^4I_{11/2}$ one remains nearly constant. This highlights the potential of highly Er^{3+}-doped Na$_5$Y$_9$F$_{32}$ crystals for laser operation in the mid-IR. Considering the deteriorated optical quality of 10 at.% Er^{3+}-doped crystals, the doping levels about 4 – 7 at.% appear to be promising for laser experiments.
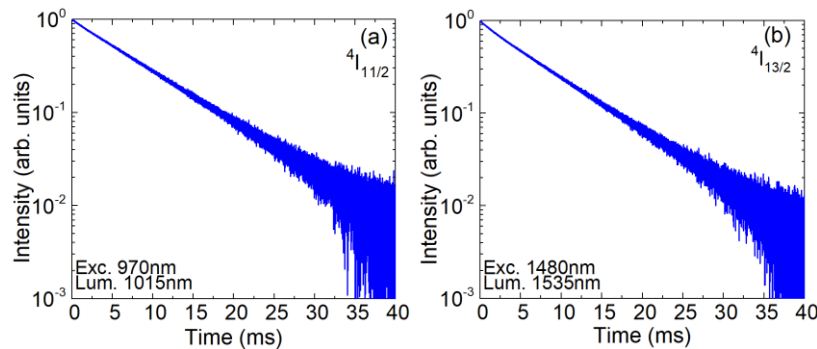

Figure 6. Luminescence decay curves for Er^{3+} ions in an 5.59 at.% Er:Na$_5$Y$_9$F$_{32}$ crystal: (a) decay from the $^4I_{11/2}$ state, λ_{exc} = 970 nm, λ_{lum} = 1015 nm; (b) decay from the $^4I_{13/2}$ state, λ_{exc} = 1480 nm, λ_{lum} = 1535 nm.

Table 2. Luminescence decay lifetimes τ_{lum} of the $^4I_{11/2}$ and $^4I_{13/2}$ Er^{3+} manifolds in Na$_5$Y$_9$F$_{32}$ as a function of doping level.

Er content (at.%)	0.22	1.16	2	5.59	9.63
τ_{lum}($^4I_{11/2}$), ms	6.78	6.55	6.65	7.72	6.41
τ_{lum}($^4I_{13/2}$), ms	10.51	10.20	8.53	6.69	3.79

4. CONCLUSIONS

To conclude, Er^{3+}-doped Na$_5$Y$_9$F$_{32}$ (5NaF·9YF$_3$) fluoride crystal is an attractive material for mid-infrared lasers emitting around 2.8 μm according to the $^4I_{11/2} \rightarrow {}^4I_{13/2}$ transition. This crystal possesses a cubic (fluorite-type) structure. The Er^{3+} ions in Na$_5$Y$_9$F$_{32}$ exhibit significant inhomogeneous spectral broadening leading to broad and smooth ("glassy-like") absorption and emission spectral bands. The low-phonon-energy behavior of the host matrix (the most intense Raman band for undoped Na$_5$Y$_9$F$_{32}$ is found at ~404 cm^{-1}) determines relatively long luminescence lifetimes of the upper laser manifold ($^4I_{11/2}$), about 6-7 ms. A favorable ratio of the upper-to-lower laser level lifetimes is reached already at moderate Er^{3+} doping levels (~5 at.%).

5. ACKNOWLEDGEMENTS

REFERENCES

[1] R. E. Thoma, G. M. Hebert, H. Insley, and C.F. Weaver, "Phase equilibria in the system sodium fluoride-yttrium fluoride," Inorg. Chem. 2(5), 1005-1012 (1963).

[2] R. E. Thoma, H. Insley, and G. M. Hebert, "The sodium fluoride-lanthanide trifluoride systems," Inorg. Chem. 5(7), 1222-1229 (1966).

[3] L. Pontonnier, S. Ale, J. J. Capponi, M. Brunel, and F. de Bergevin, "An approach to the local arrangement of the fluorine atoms in the anionic conductors with the fluorite structure $Na_{0.5-x}Y_{0.5+x}F_{2+2x}$," Solid State Ion. 9, 549-553 (1983).

[4] A. M. Tkachuk, S. E. Ivanova, and M. F. Joubert, "Luminescence self-quenching from $^4F_{3/2}$, $^2P_{3/2}$ and $^4D_{3/2}$ neodymium levels in double sodium- yttrium fluoride crystals," J. Lumin. 94-95, 343-347 (2001).

[5] N. I. Sorokin, A. K. Ivanov-Shits, L. L. Vistin, and B. P. Sobolev, "Anionic conductivity in $Na_{0.5-x}R_{0.5+x}F_{2+2x}$ (R = Dy-Lu; Y; $x \cong 0.1$) single crystals with fluorite-type structure," Kristallografiya 37(2), 421-426 (1992).

[6] N. I. Sorokin, B. P. Sobolev, and M. W. Breiter, "Anion transport in superionic conductors $Na_{0.5-x}R_{0.5+x}F_{2+2x}$ (R are cations of rare-earth elements) at elevated temperatures" Russ. J. Electrochem. 38(5), 516-521 (2002).

[7] K. Labbaci, and M. Diaf, "Crystal growth and spectroscopic investigations of Tm^{3+} ions doped $5NaF-9YF_3$ fluoride single crystals," Phys. Scr. 75(3), 327 (2007).

[8] T. Jensen, A. Diening, G. Huber, and B. H. T. Chai, "Investigation of diode-pumped 2.8-µm $Er:LiYF_4$ lasers with various doping levels," Opt. Lett. 21(8), 585-587 (1996).

[9] M. Pollnau, W. Luthy, H. P. Weber, T. Jensen, G. Huber, A. Cassanho, H. P. Jenssen, and R. A. McFarlane, "Investigation of diode-pumped 2.8-µm laser performance in $Er:BaY_2F_8$," Opt. Lett. 21(1), 48–50 (1996).

[10] L. Basyrova, P. Loiko, J. L. Doualan, A. Benayad, A. Braud, C. Labbé, and P. Camy, "$Er:KY_3F_{10}$ laser at 2.80 µm," Opt. Lett. 46(22), 5739-5742 (2021).

[11] C. Labbe, J. L. Doualan, P. Camy, R. Moncorgé, and M. Thuau, "The 2.8 µm laser properties of Er^{3+} doped CaF_2 crystals," Opt. Commun. 209(1-3), 193-199 (2002).

[12] L. Basyrova, P. Loiko, J. L. Doualan, A. Benayad, A. Braud, B. Viana, and P. Camy, "Thermal lensing, heat loading and power scaling of mid-infrared $Er:CaF_2$ lasers," Opt. Lett. 30(5), 8092-8103 (2022).

[13] A. M. Tkachuk, S. E. Ivanova, M. F. Joubert, Y. Guyot, and V. P. Gapontzev, "Population of excited erbium levels in $Er^{3+}:Na_{0.4}Y_{0.6}F_{2.2}$ (Er: NYF) laser crystals," J. Alloys Compd. 380(1-2), 130-135 (2004).

[14] C. Labbé, J. L. Doualan, S. Girard, and P. Le Boulanger, "The excited state absorption of $Er^{3+}:LiYF_4$ and $Er^{3+}:Na_5Y_9F_{32}$," J. Alloys Compd. 275, 264-268 (1998).

[15] W. T. Carnall, P. R. Fields, and K. Rajnak, "Electronic energy levels in the trivalent lanthanide aquo ions. I. Pr^{3+}, Nd^{3+}, Pm^{3+}, Sm^{3+}, Dy^{3+}, Ho^{3+}, Er^{3+}, and Tm^{3+}," J. Chem. Phys. 49(10), 4424-4442 (1968).

[16] B. R. Judd, "Optical absorption intensities of rare-earth ions," Phys. Rev. 127(3), 750-761 (1962).

[17] G. S. Ofelt, "Intensities of crystal spectra of rare-earth ions," J. Chem. Phys. 37(3), 511-520 (1962).

[18] B. F. Aull and H. P. Jenssen, "Vibronic interactions in Nd:YAG resulting in nonreciprocity of absorption and stimulated emission cross sections," IEEE J. Quantum Electron. 18(5), 925-930 (1982).